

Segmentation of Abdominal Aortic Aneurysm (AAA) Based on Topology Prior Model

Safa Salahat¹(✉), Ahmed Soliman², Tim McGloughlin³,
Naoufel Werghi¹, and Ayman El-Baz²

¹ Electrical and Computer Engineering Department, Khalifa University,
Abu Dhabi, United Arab Emirates

{safa.salahat, naoufel.werghi}@kustar.ac.ae

² BioImaging Laboratory, Bioengineering Department, University of Louisville,
Louisville, KY, USA

{ahmed.soliman, ayman.elbaz}@louisville.edu

³ Biomedical Engineering Department, Khalifa University,
Abu Dhabi, United Arab Emirates

tim.mcgloughlin@kustar.ac.ae

Abstract. In this paper, we propose a statistical based method using a topology prior model, integrating both intensity and shape information, to segment abdominal aortic aneurysm (AAA) from computed tomography angiography (CTA) scans. The method was tested on a total of 48 slices taken from 6 different patients and has shown competitive performance compared with the best reported results in the literature. Our method has achieved a mean Dice coefficient of $0.9303_{\pm 0.0499}$, and mean Hausdorff distance of $3.5703_{\pm 3.1941}$ mm. This method overcomes the major problem faced by currently existing solutions of similar Hounsfield values of neighboring tissues to that of the AAA thrombus. This is a promising medical tool which can be used to analyze the AAA in order to generate an accurate rupture risk indicator.

Keywords: Abdominal aortic aneurysm · Segmentation · Lumen · Thrombus · Topology · Probability

1 Introduction

Abdominal Aortic Aneurysm (AAA) is a balloon like dilation in abdominal aorta which may lead to patient death if untreated. The expansion is defined as an aneurysm if its maximum diameter reaches 3 cm, and usually requires medical intervention when the maximum diameter reaches 5.5 cm [1–3]. Currently, there are two techniques used for aneurysm repair, open aneurysm repair (OR) and Endovascular Aneurysm Repair (EVAR). In the former, the aneurysm is replaced with a graft, and in the later, a stent graft is inserted inside the aneurysm lumen to avoid the invasive open surgery [4].

Lumen, thrombus, calcification and vessel wall are the components of the aneurysm, as illustrated in Fig. 1. Currently, clinicians' rupture risk assessment is mainly based on the maximum measured diameter of the aneurysm. However, some studies have indicated that AAA maximum diameter doesn't always lead to accurate prediction

of rupture risk [5, 6]. Several contributions from biomechanics have suggested that peak wall stress can predict rupture risk [7–10]. It is also important for surgery planning and accurate patient-specific stent graft fabrication. Segmentation of the aneurysm and extraction of the lumen and the thrombus are required tasks for the aforementioned purposes. Manual segmentation of the aneurysm is a time consuming task for the clinicians. Considering the high number of patients diagnosed with AAA on daily basis worldwide, there is a need to develop automated methods to segment the aneurysm.

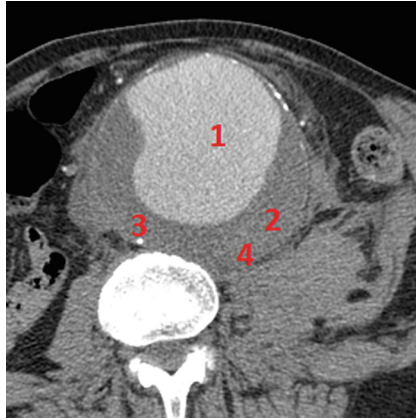


Fig. 1. The four main components of an AAA. The region labeled with 1 is the lumen, while the darker region labeled with 2 is the thrombus. The bright spots around the aneurysm labeled as region 3 are the calcified regions. Label 4 represents the vessel wall.

In response to this need, numerous contributions from the medical imaging community have been proposed providing fully and semi-automated solutions for the AAA segmentation problem. These efforts have mostly concentrated on the lumen and thrombus segmentation, and have relied on deformable models, graph cut, fuzzy c-means clustering, or a combination of other methods to perform the AAA segmentation.

While the problem of lumen segmentation is relatively easy due to the contrast agent injected into the patient which makes the lumen distinguishable from other structures, the segmentation of the thrombus is more challenging since Hounsfield values which represent it are very similar to other neighboring structures which results in weak edges. Further, other organs with strong features, e.g. spinal cord, and presence of calcification may obstruct the segmentation of the thrombus. In addition, the aneurysm doesn't have a specific shape or geometry to aid in the segmentation of the thrombus.

Most of the proposed solutions for aneurysm segmentation are based on deformable models [11–21]. However, this class of solutions has three major weaknesses. Deformable models are more computationally demanding than other methods, the outer edge of the aneurysm is of weak gradient which results in over- or under-segmentation of the aneurysm, and these models can easily get drawn to other structures of high gradient. Therefore, extra stopping criteria, and/or approximate shape constraints are added to the models to improve the results. In addition, some user interaction, other

commercial software, or preprocessing step(s) may be needed to remove these structures before the segmentation process starts.

Graph cut based methods also over-segments the aneurysm and includes other structures in addition to it [22–25]. Shape constraint or further analysis is needed to exclude irrelevant regions.

Fuzzy c-means based solutions [26, 27] generate a binary image of all organs in a CT scan, and the result obtained is highly dependent on threshold and other tuned parameters values used. It is also observed that fuzzy c-means cannot distinguish between the thrombus and neighboring tissues of similar Hounsfield values.

Some other contributions utilized low level image processing operations such as thresholding and morphological operation [28], region growing [29, 30], isoperimetric segmentation [31], histogram derived information [32], active learning and random forest classifier [33, 34]. These methods are dependent on user interaction, threshold and parameters tuned, and aneurysm shape fitting into a mathematical shape (e.g. ellipse, circle, or radial function) into the thrombus.

In summary, it is clear that currently existing solutions has one or more of the following three problems: (1) The method cannot fully/partially distinguish the thrombus from other tissues, (2) The segmentation is hindered by other structures of strong features, (3) Computationally demanding, (4) Extra user interaction is needed to guide the segmentation process, or correct it afterwards.

Therefore, it is desirable to develop a robust solution which tackles the above mentioned drawbacks. In this work, we employ a statistical topology prior model based method which utilizes both intensity and shape information to segment thrombus and lumen volumes from CT data. This method is used for the first time to solve the AAA segmentation problem, and have managed to overcome the above mentioned limitations to a great extent while maintaining high accuracy at the same time.

The remaining of the paper is organized as follows. Section 2 describes the methodology used for aneurysm segmentation. Section 3 provides a detailed evaluation and analysis of the results obtained. Section 4, concludes the paper.

2 Methodology

The proposed framework for segmenting the AAA thrombus and the lumen from 3D-CT data (depicted in Fig. 2) utilizes a label propagation, with topology preservation, scheme using both a patient specific shape model and 1st order adaptive intensity model to overcome the problem of intensity homogeneity between thrombus and its adjacent structures. Details of each model component are as follow.

2.1 Patient Specific Shape Model

Accurate segmentation of the Abdominal Aortic Aneurysm (AAA) wall is very difficult since the intensities/grey levels of the AAA wall are very close to the intensities of other abdominal tissues. Thus, inclusion of information on the shape or topology of AAA wall will provide a guiding feature during the segmentation process and

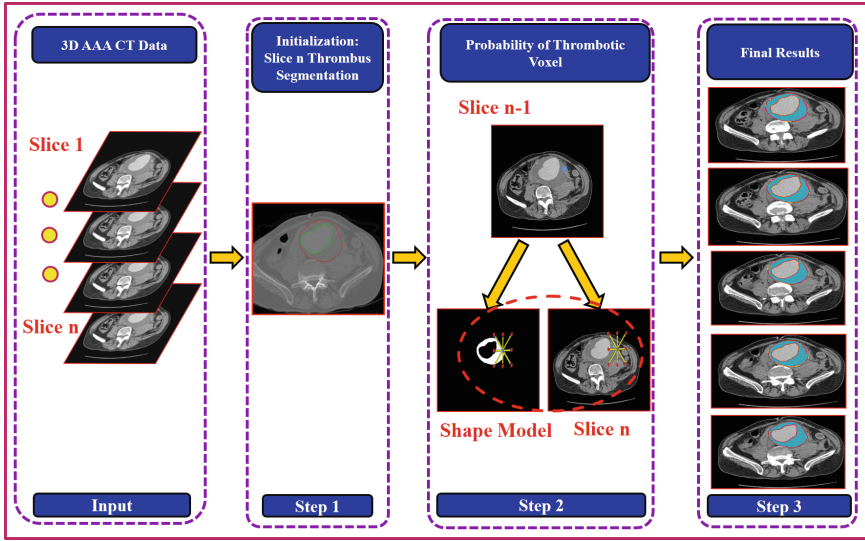


Fig. 2. Block diagram of the AAA segmentation.

potentially enhance the segmentation accuracy. The primary challenge in creating a prior shape model of the AAA wall is the high intra-patient variability, especially due to pathology. To overcome this challenge, in this manuscript, we are introducing adaptive shape-specific model that is based on manual delineation of the inner and outer borders of AAA. Subsequently, the appearance and the topology of manually segmented AAA wall will be used to guide the segmentation of the adjacent slice. Each slice segmentation will drive its adjacent one which can be viewed as an adaptive label propagation process (see Fig. 3).

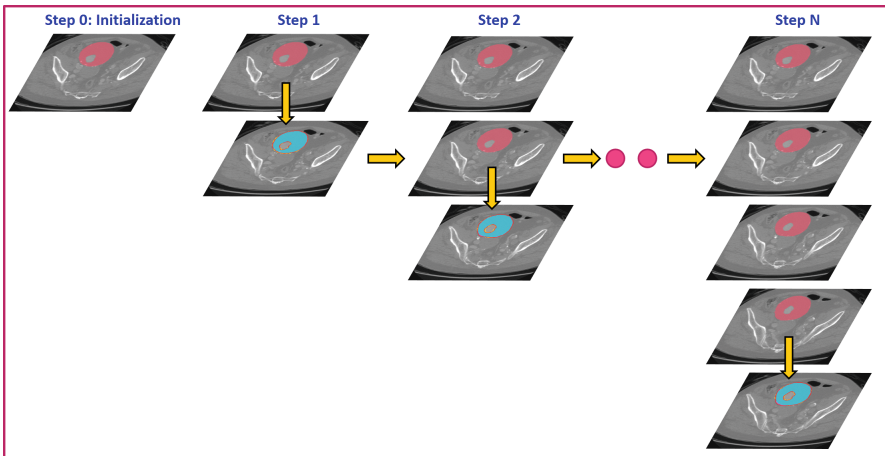


Fig. 3. Step-by-step illustration of the guiding shape model.

2.2 1st Order Adaptive Intensity Model

Unlike traditional shape models that depends only on the mapped voxel location to calculate the probabilistic map, our 1st order adaptive intensity model ensures that only the visually similar voxels will contribute in the probability map calculations for the slice to be segmented to provide an accurate segmentation results.

The complete framework proceeds as follows: Starting from the last slice, the lumen and the thrombus of the last slice are manually segmented by the operator, which results in two binary masks which are subtracted to produce the binary mask representing the thrombotic region in the last slice (see Fig. 4). (2) Then moving backward, each slice i is segmented referring to the previously segmented slice $(i + 1)$. This procedure is performed as follows: at each voxel in the slice i an $N1 \times N2$ window w is generated around its counterpart in slice $(i + 1)$, then voxels in that window whose Hounsfield values fall within a predefined tolerance $\pm\tau$ are select. If no voxels are found, window size is increased until such voxel(s) are found, or maximum window size is reached. (4) Then the probability of each voxel to be part of the thrombus is calculated as the occurrence of positively labeled voxels from the total voxels in slice $i + 1$ which are within the window whose Hounsfield values are close to the voxel in slice i . Therefore, if we have k similar voxels within the window, of which m are labeled as 1, then the probability of this voxel in slice i to belong to the thrombus is simply $p_{TH}(x) = m/k$. If $(p_{TH}(x) > p_{BG}(x))$ then this voxel x belongs to the thrombus, and background otherwise. (5) 2D median filter

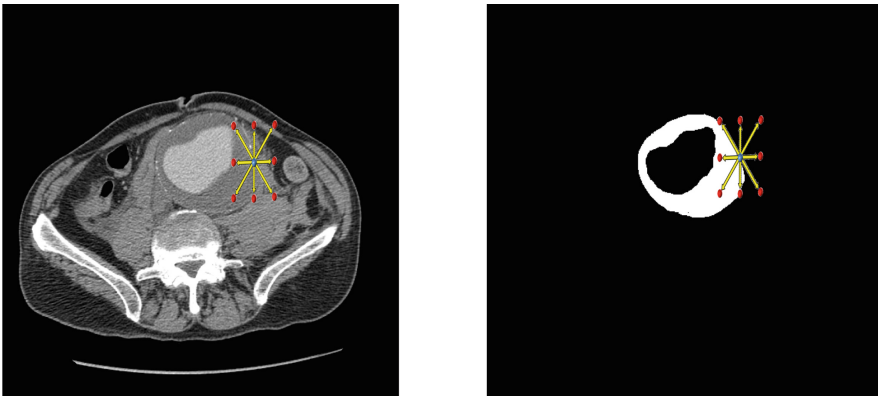


Fig. 4. Slice n and its binary mask resulting from the manual segmentation.

For example, in a 3×3 window, if k voxels in slice n are similar to voxel x (in slice $n-1$) Hounsfield value (within the given tolerance), and m out of these k voxels are labeled as 1, then $p_{TH}(x) = m/k$. The related algorithm of the above procedure can be described in more details as follows:

Algorithm 1:- Topology based segmentation

1. Manually label the outer boundaries of the lumen and the thrombus in slice n .
 2. Derive a masks related to the thrombotic region labeled as 1 for thrombotic voxel and 0 for background.
 3. For each slice i , $i=n-1$ to 1
 - I. For each voxel x in slice i
 - a) Construct a window w around the counterpart of voxel x in slice $i+1$
 - b) Find voxels within with Hounsfield values that fall within a predefined tolerance $\pm\tau$ in w
 - c) If no voxels are found to satisfy (e), increase size of w until correspondences are found or the maximum size allowed for w is reached
 - d) Calculate the probability $p(x)$ of each voxel belonging to the thrombus based on the occurrences of white voxels from the total corresponding voxels which satisfy (e) in slice $i+1$.
 - e) If $(p_{th}(x) > p_{bg}(x))$, x is part of the thrombus, background otherwise.
- End For
- End For
4. Apply 3D smoothing using 3D median filter on the reconstructed 3D volume
-

Filter is then applied for each slice independently to improve the 2D segmentation result. (6) The whole volume is finally reconstructed, and 3D-median filter is applied to the volume improve segmentation consistency and surface smoothness. The final result is a binary volume which labels the thrombus across the slices.

3 Method Evaluation

This method has been tested on CT datasets collected from six patients, the region of interest to be segmented appears in eight slices each, who diagnosed with AAA which was provided by Limerick University. The in-plane voxel spacing ranges from 0.7031×0.7031 to 0.8984×0.8984 , while the slice thickness ranges from 1.25 mm to 5 mm. Final results obtained are visualized in Fig. 4. To evaluate the accuracy of our method, we have used the Dice similarity coefficient (DC) and Hausdorff distance, that characterize the spatial overlap and surface-to-surface distances, in addition to other commonly used metrics, for comparison purpose, as illustrated in Table 1. An expert radiologist manually labeled the thrombus and the lumen of the aneurysm to acquire the ground truth data to be utilized to evaluate the accuracy of our proposed method.

Figure 5 shows a 2D axial projection for sample results obtained by our proposed method, from different subjects, where the ground truth edges are plotted in red along our segmentation in addition to false positive and false negative (in green, yellow, and pink respectively). It is clear from the sample results in Fig. 5 that our proposed method accurately segment the thrombus from its neighbors with little false positive segmentation as a result of high homogeneity of neighboring tissues. This proposed method managed to achieve results which are comparable to best results reported in the literature. The mean dice coefficient obtained was $0.9303_{\pm 0.0499}$, and mean thrombus Hausdorff distance was $3.5703_{\pm 3.1941}$. Our results are summarized in Table 1. To provide a comparison with the best results from the literature, we used all the accuracy

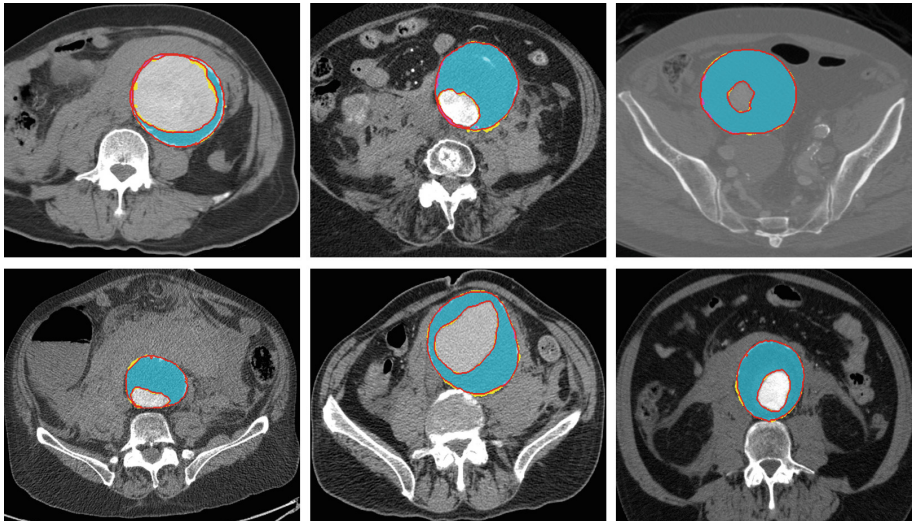


Fig. 5. Example thrombus segmentation result taken from different patients with color-coded ground truth edges, false positive errors, and false negative errors (red, yellow, and pink, respectively). (Color figure online)

Table 1. Evaluation of the proposed thrombus segmentation method tested on the six patients.

Metric	Mean \pm Std
Dice coefficient	$0.9303_{\pm 0.0499}$
Sensitivity	$0.9138_{\pm 0.0621}$
Specificity	$0.9989_{\pm 0.0005}$
Positive predictive value	$0.9483_{\pm 0.0438}$
Volume overlap %	$87.35_{\pm 8.180}$
Hausdorff distance (mm)	$3.5703_{\pm 3.1941}$
Mean absolute surface distance (mm)	$0.2578_{\pm 0.2274}$
Mean absolute volume difference %	$5.3665_{\pm 2.3786}$
Mean symmetric absolute surface distance	$0.4752602_{\pm 0.4119}$

Table 2. Best literature reported thrombus segmentation results

Reference	Metric	Value	Slices/patients
12	Dice coefficient	0.8508 to 0.9316	7/-
11	Sensitivity	0.9354	5/-
11	Specificity	0.9837	5/-
35a	Volume overlap %	95 ± 3.30	125/17
23	Outer wall Hausdorff distance (mm)	3.09 ± 1.81	24/-
22	Mean unsigned error for thrombotic surface (mm)	1.9 ± 0.72	1300/9
25	Mean absolute volume difference %	8.0 ± 7.00	-/8
25	Average symmetric surface distance	1.46 ± 0.40 mm	-/8

In this reference, the metric is referred as Volume overlap but, in our opinion, it seems rather as Dice coefficient.

metrics used by all the compared work, illustrating total number of slices and/or patients used for testing, are provided in Table 2. The most important parameters which affect the segmentation result are the tolerance τ , which controls the voxels that will contribute in the current voxel probability calculation, and the maximum window size, which determines the search space for these voxels.

The test set used in [11, 12] is very limited. Although the testing was performed on a large dataset in [22], it requires several manual initializations and user guidance throughout the segmentation process, which explains the high performance obtained. It can be observed that our results surpasses the best results reported in the literature for some metrics, and produce comparable results for others, except for the volume overlap metric where our method is approximately 7.65% less than the highest reported value.

4 Conclusion

In conclusion, this paper has suggested a new statistical-based method for Abdominal Aortic Aneurysm segmentation from 3D-CT which utilizes topology (both intensity and shape) information to perform the segmentation. Results obtained are competitive to the best results reported in literature. This makes it a promising robust medical tool to perform aneurysm segmentation to reduce the burden on radiologists. In future, we will perform testing on a larger data set, and aim to detect the calcification which exits within the aneurysm to complete the final objective of building a biomechanical model which works as a rupture risk indicator.

Acknowledgements. This research was funded with a generous grant from Al-Jalila Foundation, Grant no. AJF201551. Ethics approval from University of Limerick, Ireland was acquired for the used data set in this research.

References

1. Moll, F., et al.: Management of abdominal aortic aneurysms clinical practice guidelines of the european society for vascular surgery. *Eur. J. Vasc. Endovasc. Surg.* **41**(1), 1–58 (2011)
2. Ernst, C.B.: Abdominal aortic aneurysms. *N. Engl. J. Med.* **328**(16), 1167–1172 (1993)
3. Vardulaki, K.A., et al.: Growth rates and risk of rupture of abdominal aortic aneurysms. *Br. J. Surg.* **85**(12), 1674–1680 (1998)
4. Zarins, C.K., et al.: AneuRx stent graft versus open surgical repair of abdominal aortic aneurysms: multicenter prospective clinical trial. *J. Vasc. Surg.* **29**(2), 292–305 (1999)
5. Darling, R.C., Messina, C.R., Brewster, D.C., Ottinger, L.W.: Autopsy study of unoperated abdominal aortic aneurysms. The case for early resection. *Circulation* **56**(3), 161–164 (1977)
6. Conway, K.P., Byrne, J., Townsend, M., Lane, I.F.: Prognosis of patients turned down for conventional abdominal aortic aneurysm repair in the endovascular and sonographic era: Szilagyi revisited? *J. Vasc. Surg.* **33**(4), 752–757 (2001)
7. Georgakarakos, E., et al.: The role of geometric parameters in the prediction of abdominal aortic aneurysm wall stress. *Eur. J. Vasc. Endovasc. Surg.* **39**(1), 42–48 (2010)
8. Venkatasubramaniam, A.K., et al.: A comparative study of aortic wall stress using finite element analysis for ruptured and non-ruptured abdominal aortic aneurysms. *Eur. J. Vasc. Endovasc. Surg.* **28**(2), 168–176 (2004)
9. O’Leary, S.A., et al.: Determining the influence of calcification on the failure properties of abdominal aortic aneurysm (AAA) tissue. *J. Mech. Behav. Biomed. Mater.* **42**, 154–167 (2015)
10. Vorp, D.A., Raghavan, M.L., Webster, M.W.: Mechanical wall stress in abdominal aortic aneurysm: influence of diameter and asymmetry. *J. Vasc. Surg.* **27**(4), 632–639 (1998)
11. Demirci, S., Lejeune, G., Navab, N.: Hybrid deformable model for aneurysm segmentation. Boston, 28 June–1 July 2009
12. Das, B., Mallya, Y., Srikanth, S., Malladi, R.: Aortic thrombus segmentation using narrow band active contour model. New York, August–3 September 2006
13. Zohiosia, C., Kossiorisa, G., Papaharilaou, Y.: Geometrical methods for level set based abdominal aortic aneurysm thrombus and outer wall 2D image segmentation. *Comput. Methods Programs Biomed.* **107**(2), 202–217 (2012)
14. Subašić, M., Lončarića, S., Sorantin, E.: Model-based quantitative AAA image analysis using a priori knowledge. *Comput. Methods Programs Biomed.* **80**(2), 103–114 (2005)
15. Loncaric, S., Subasic, M., Sorantin, E.: 3-D deformable model for aortic aneurysm segmentation from CT images, Chicago, IL, 23–28 July 2000
16. Loncaric, S., Subasic, M., Sorantin, E.: 3-D deformable model for abdominal, 23–28 July 2000
17. Subasic, M., Loncaric, S., Sorantin, E.: 3-D Image Analysis of Abdominal Aortic Aneurysm. San Diego, CA (2001)
18. Subasic, M., Loncaric, S., Sorantin, E.: Region-based deformable model for aortic wall segmentation, Rome, 18–20 September 2003
19. Magee, D., Bulpitt, A., Berry, E.: Level set methods for the 3D segmentation of CT images of abdominal aortic aneurysms, pp. 141–144 (2001)
20. Bulpitt, A.J., Berry, E.: Spiral CT of abdominal aortic aneurysms: comparison of segmentation with an automatic 3D deformable model and interactive segmentation, San Diego (1998)
21. Magee, D., Bulpitt, A., Berry, E.: Combining 3D deformable models and level set methods for the segmentation of abdominal aortic aneurysms, Manchester (2001)

22. Lee, K., et al.: Three-dimensional thrombus segmentation in abdominal aortic aneurysms using graph search based on a triangular mesh. *Comput. Biol. Med.* **40**(3), 271–278 (2010)
23. Duquette, A.A., Jodoin, P.-M., Bouchot, O., Lalande, A.: 3D segmentation of abdominal aorta from CT-scan and MR images. *Comput. Med. Imaging Graph.* **36**(4), 294–303 (2012)
24. Hraiech, N., Carroll, M., Rochette, M., Coatrieux, J.L.: 3D vascular shape segmentation for fluid-structure modeling, Lyon, 13–15 June 2007
25. Freiman, M., Esse, S.J., Joskowicz, L., Sosna, J.: An iterative model-constrained graph-cut algorithm for abdominal aortic aneurysm thrombus segmentation. Rotterdam, 14–17 April 2010
26. Pham, T.D., Golledge, J.: Geostatistically constrained fuzzy segmentation of abdominal aortic aneurysm CT Images, Hong Kong, 1–6 June 2008
27. Majd, E.M., Sheikh, U.U., Abu-Bakar, S.A.R.: Automatic segmentation of abdominal aortic aneurysm in computed tomography images, Kuala Lumpur, 15–18 December 2010
28. Dehmeshki, J., et al.: Computer aided detection and measurement of abdominal aortic aneurysm using computed tomography digital images, Cancun, February 2009
29. Biasi, H.D., Wangenheim, A.V., Silveira, P.G., Comunello, E.: 3D reconstruction of abdominal aortic aneurysms, Maribor (2002)
30. Macía, I., Legarreta, J.H., Paloc, C., Graña, M., Maiora, J., García, G., Blas, M.: Segmentation of abdominal aortic aneurysms in CT images using a radial model approach. In: Corchado, E., Yin, H. (eds.) *IDEAL 2009*. LNCS, vol. 5788, pp. 664–671. Springer, Heidelberg (2009). doi:[10.1007/978-3-642-04394-9_81](https://doi.org/10.1007/978-3-642-04394-9_81)
31. Bodur, O., et al.: Semi-automatic aortic aneurysm analysis, San Jose (2007)
32. Hosseini, B., et al.: Automatic segmentation of abdominal aortic aneurysm using logical algorithm. Pisa, 17–19 November 2010
33. Maiora, J., Ayerdi, B., Graña, M.: Random forest active learning for AAA thrombus segmentation in computed tomography angiography images. *Neurocomputing* **126**, 71–77 (2014)
34. Maiora, J., Graña, M.: Abdominal CTA image analysis through active learning and decision random forests: application to AAA segmentation, Brisbane, 10–15 June 2012